

The effect of low dose rate on metabolomic response to radiation in mice

Maryam Goudarzi · Tytus D. Mak ·
Congju Chen · Lubomir B. Smilenov ·
David J. Brenner · Albert J. Fornace

Received: 4 April 2014 / Accepted: 8 July 2014
© Springer-Verlag Berlin Heidelberg 2014

Abstract Metabolomics has been shown to have utility in assessing responses to exposure by ionizing radiation (IR) in easily accessible biofluids such as urine. Most studies to date from our laboratory and others have employed γ -irradiation at relatively high dose rates (HDR), but many environmental exposure scenarios will probably be at relatively low dose rates (LDR). There are well-documented differences in the biologic responses to LDR compared to HDR, so an important question is to assess LDR effects at the metabolomics level. Our study took advantage of a modern mass spectrometry approach in exploring the effects of dose rate on the urinary excretion levels of metabolites 2 days after IR in mice. A wide variety of statistical tools were employed to further focus on metabolites, which showed responses to LDR IR exposure (0.00309 Gy/min) distinguishable from those of HDR. From a total of 709 detected spectral features, more than 100 were determined to be statistically significant when comparing urine from mice irradiated with 1.1 or 4.45 Gy to that of sham-irradiated mice 2 days post-exposure. The

results of this study show that LDR and HDR exposures perturb many of the same pathways such as TCA cycle and fatty acid metabolism, which also have been implicated in our previous IR studies. However, it is important to note that dose rate did affect the levels of particular metabolites. Differences in urinary excretion levels of such metabolites could potentially be used to assess an individual's exposure in a radiobiological event and thus would have utility for both triage and injury assessment.

Keywords Metabolomics · Low dose rate radiation · Mass spectrometry

Introduction

The adverse effects of radiation exposure are well known and have been extensively documented in radiologic disaster cases such as Chernobyl, and more recently, Fukushima, as well as in the earlier A-bomb nuclear events. During nuclear catastrophic events, people in the immediate disaster zone will incur acute exposures at high dose rates (HDR), but many will experience exposure to low dose rate (LDR) radiation from fallout, groundshine, and internal emitters. In the case of radiologic events, much of the exposure may well be categorized as LDR. Although the damaging health effects of exposure to high doses of radiation at HDR are well documented, more work needs to be done to establish a biologic signature for exposure to low dose rates (LDR). Previous studies have shown that exposure to LDR radiation reduces cell killing compared with a single dose of HDR radiation (Elkind and Sutton 1959; Oakberg and Clark 1961), as also shown in separate split-dose experiments. This is probably due to the ability of cells to continually repair damage, such as double-strand

Electronic supplementary material The online version of this article (doi:10.1007/s00411-014-0558-1) contains supplementary material, which is available to authorized users.

M. Goudarzi · A. J. Fornace
Biochemistry and Molecular and Cellular Biology, Georgetown University, Washington, DC, USA

T. D. Mak · A. J. Fornace (✉)
Lombardi Comprehensive Cancer Center, Georgetown University, Washington, DC, USA
e-mail: Af294@georgetown.edu

C. Chen · L. B. Smilenov · D. J. Brenner
Center for High-Throughput Minimally-Invasive Radiation Biodosimetry, Columbia University, New York, NY, USA

breaks, at lower dose rates so that the level of damage at any one time is low (Evans et al. 1985; Nagasawa et al. 1992).

There remains the need to study the effects of LDR exposure *in vivo* and to determine its distinct effects and biologic signatures in easily obtainable fluids to more closely mimic the potential environmental exposures of individuals. At lower doses, it is also important to be able to detect slight changes in the composition of biofluids, which can potentially identify those subjects who are at higher long-term risk of cancer and other sequela. Advances in mass spectrometry have allowed for high-throughput accurate detection of changes in biofluids. This technology was employed in this study to detect distinct and subtle changes in the urinary excretion of metabolites from mice exposed to LDR and HDR irradiation. These changes represent IR-induced injury, which will be manifested in perturbation of metabolic pathways. In this study, we focused on establishing a metabolomic profile for urine obtained from mice exposed to 4.45 and 1.1 Gy at LDR (0.00309 Gy/min) and compared it to that of mice exposed to the same doses at HDR (1.03 Gy/min). The objective of this study was to determine early markers for LDR exposure at 4.45 Gy, which would show persistent changes even at the lower dose of 1.1 Gy. It is important to develop early biomarkers, as LDR exposure to fallout and internal emitters will occur over an extended period of time. We have already shown a clear metabolomic response to an internal emitter (Goudarzi et al. 2013). In this study, we focused on establishing a metabolomic profile for HDR exposure and LDR exposure to highlight their subtle differences, as well as similarities using a wide array of statistical tools. This may shed light on the different pathways perturbed the most by dose rate. Our results in this initial LDR study will help develop a more accurate predictor of radiation injury, which in turn should impact patient triage and treatment on an individual basis in case of a radiologic or nuclear disaster.

Materials and methods

Chemicals

Debrisoquine sulfate, pantothenic acid, indole-3-carboxylic acid, 5-hydroxy-L-tryptophan, kynurenic acid, riboflavin, and 4-nitrobenzoic acid (4-NBA) were purchased from Sigma Chemical Company (St. Louis, MO). N1-methyl-2-pyridone-5-carboxamide and phenylacetylglycine were obtained from Santa Cruz Biotechnology, Inc. (Santa Cruz, CA). The UPLC-grade solvents were purchased from Fisher Scientific (Hampton, NH).

Animals

All animal husbandry and experimental procedures were conducted in accordance with applicable federal and state guidelines and approved by the Animal Care and Use Committee of Columbia University Medical Center. Male C57BL/6N mice, aged 8–10 weeks old, were obtained from Charles River Laboratories, Inc. (Wilmington, MA). Mice were housed at Columbia University animal facility under standard 12 h light and 12 h dark cycle conditions and given water and regular rodent chow *ad libitum*. Animals were 8–9 weeks of age when they were exposed to IR. For total body acute irradiations, the mice were placed in a box with a size of 6 cm (*W*), 12.5 cm (*L*), and 8 cm (*H*) containing bedding and irradiated in the X-ray machine (X-Rad 320, Precision X-Ray Inc, Branford, CT) with a dose rate of 1.03 Gy/min. For total body LDR irradiations, the mice were placed in a specially designed mouse box, consisting of four compartments with a size of 6 cm (*W*), 12.5 cm (*L*), and 8 cm (*H*). Each compartment was supplied with bedding, water (from water bottle), and food (gel-packs). Before the irradiation, the mice were acclimated to the mouse compartments for 24 h. For irradiation, the box with the mice was placed in the X-ray machine and the following conditions were maintained during the irradiation: (1) light conditions: 12 h light/dark cycle, (2) temperature and humidity: The temperature in the X-ray machine was maintained at 22 °C (\pm 0.5 °C) and the humidity at 30–40 % by using a portable custom air conditioning system, (3) air exchange: A fan (Nuline, #: 04424883) mounted over one of the service ports of the X-ray machine maintained more than 10 air exchange volumes per hour. Mice were monitored through the door window of the X-ray machine. The behavior of the animals was normal, and they followed their usual cycle of sleeping, feeding, and activity. LDR irradiation was at a dose rate of 0.00309 Gy/min. This experiment was carried out in two phases. In the first phase of the experiment, four mice were placed in each study group (control, HDR, and LDR) to establish a robust urinary metabolomic response to irradiation and dose rate. In the second phase, an independent validation experiment was carried out in the same manner and under the same conditions with four mice per group. The results of the first experiment were then confirmed in the second experiment.

This study focused on the effects of dose rate; thus, an important requirement is that both HDR and LDR irradiations should be performed using the same quality of X-rays. This must be achieved while changing only the mA and source-to-surface distance (SSD). The most able manufacturer-provided filter gives \sim 1.1 Gy/min at 50 cm SSD but a minimum of 7 Gy/day at maximum SSD. Therefore, we have created a custom Thoraeus filter

(1.25 mm Sn, 0.25 mm Cu, 1.5 mm Al) that was used for the study. This filter provides a dose rate of 1.03 Gy/min at 40 cm SSD and 3.09 mGy/min at the maximum SSD.

Urine collection

For urine collections, specifically designed metabolic cages (Techniplast USA, Exon, PA) were used. To reduce stress, the mice were acclimated to the metabolic cages for two urine collections of 24 h each prior to irradiation. After irradiation, each mouse was placed in a single metabolic cage and urine samples were collected over a period of 24 h at day 2 and day 5 post-irradiation. Urine samples were stored at -80°C until further use.

Sample preparation and mass spectrometry analysis

Urine samples were prepared as described previously by our group (Laiakis et al. 2012). Briefly, urine was diluted 1:4 in a 50 % acetonitrile solution containing 30 μM of 4-nitrobenzoic acid and 2 μM of debrisoquine. The samples were centrifuged at maximum speed to precipitate the proteins. A 5- μL aliquot of the recovered supernatant was then injected into a reverse-phase 50 \times 2.1 mm Acquity 1.7- μm C18 column (Waters Corp, Milford, MA) coupled to a time-of-flight mass spectrometry (TOFMS). The 10-min-long mobile-phase gradient switched from 100 % aqueous solvent to 100 % organic at a flow rate of 0.5 mL/min, as previously published (Laiakis et al. 2012). The QTOF Premier mass spectrometer was operated in positive (ESI⁺) and negative (ESI⁻) electrospray ionization modes. The samples were run in triplicate (technical replicates) to increase the confidence in the relative abundances of urinary ions and as a measure of reproducibility. The MS data were acquired in centroid mode and processed using MassLynx software (Waters Corp, Milford, MA).

Data processing

As described previously (Laiakis et al. 2012), MarkerLynx software (Waters Corp, Milford, MA) was used to construct a data matrix consisting of retention time, m/z , and the abundance value (via the normalized peak area) for each ion using the raw MS chromatograms. In case of the urine samples, the abundance value of each ion was normalized with respect to the total ion count (TIC) of creatinine at m/z of 114.0667 ($[\text{M} + \text{H}]^+$) and retention time of 0.32 min in each urine sample.

An in-house statistical algorithm called Metabolyzer (Mak et al. 2014) was used along with SIMCA-P+ (Umetrics, Umea, Sweden) and Random Forests (RF) to determine the metabolites that contributed the most to the differentiation between urinary profiles of irradiated

samples and that of the controls in LDR and HDR groups. When comparing data from control versus radiation-exposed animals, metabolites with non-zero abundance values in at least 70 % of samples in both groups (complete-presence ions) were first identified. The data were then log-transformed and analyzed for statistical significance via the parametric Welch's t test for statistical significance (p value <0.05). Statistical significance for ions with non-zero abundance values in at least 70 % of the samples in only one group (partial-presence ions) was analyzed categorically for differential presence status (i.e., non-zero abundance) via Fisher's exact test (p value <0.05). Only ions that fell below the p value threshold were chosen for further analysis. The log-transformed data for statistically significant complete-presence ions were then utilized for principal component analysis via singular value decomposition after zero centering and unit variance scaling. In addition, kernel principal component analysis utilizing a third-degree polynomial kernel was also conducted via the 'kernlab' package for R .

Metabolic pathway analysis

Statistically significant ions were putatively identified via Metabolyzer, which utilizes the Human Metabolome Database (HMDB) and the Kyoto Encyclopedia of Genes and Genomes (KEGG) database (Kanehisa and Goto 2000). The m/z values were used to putatively assign identities to the ions considering the possible adducts, H^+ , and Na^+ in the positive mode, and H^- and Cl^- in the negative mode. The masses were then compared to the exact mass of small molecules in the databases from which putative metabolites were identified (with a mass error of 20 ppm or less). KEGG annotated pathways associated with these putative metabolites were also identified. Selected metabolites from these pathways were later validated via MS/MS as described below.

MS/MS validation of select metabolites

Putative identity of the selected metabolites was further investigated using a more stringent monoisotopic mass error window of 7 ppm to narrow down the possibilities and increase our chance of positively identifying the chemical structure of each of the selected metabolites. The retention time of each metabolite was considered to narrow down the possibilities of the putative identifications. Several of the putatively identified metabolites ($p < 0.05$, Welch's t test) were then chosen based on their biologic relevance for further MS/MS validation against commercially available pure standards. Q-TOFMS Premier with ramping collision energy between 5 and 55 eV was used as described previously (Laiakis et al. 2012) to create MS/MS

fragmentation pattern for the selected metabolites, which were then compared to that of pure chemicals for validation purposes. Chemical standards were spiked in urine samples at known concentrations against which the intensities of urine metabolites were standardized.

Results

As described below, creatinine-normalized data were used to establish a robust metabolomic signature for urine from mice exposed to doses of 4.45 and 1.1 Gy LDR radiation. Creatinine normalization has been widely accepted and was practiced in this study because the total excretion of this ion remained relatively unchanged in irradiated and control mice across all samples. For instance, creatinine relative intensity in the control mice over the course of the study was 32.87 ± 1.87 , and for the HDR and LDR mice, these values were 34.60 ± 1.39 and 34.20 ± 1.04 , respectively. The normalized data were then analyzed using traditional statistical tools such as SIMCA-P⁺, Random Forests (RF), and Metabolyzer (Mak et al. 2014) to determine whether the urinary metabolomic profile of LDR-irradiated mice could be distinguished from that of HDR-irradiated mice at matching doses. Although LDR and HDR share many similarities in their urinary metabolomic profiles, subtle and unique differences were observed with dose rate. Furthermore, the urinary profile of each dose rate was then studied over time to look for persistent IR effects.

Dose rate response

Metabolyzer was initially used to determine whether the metabolomic signature of urine from mice collected 2 days after 4.45 Gy irradiation was distinguishable from that of control samples in both LDR and HDR cases. We initially chose data from mice exposed to 4.45 Gy irradiation to establish a metabolomic signature for 4.45 Gy HDR irradiation and 4.45 Gy LDR irradiation. Later, we selected metabolites that contributed most significantly to establishing the metabolomic signatures of HDR and LDR irradiation. We also explored the robustness of responses from the selected metabolites at a lower dose of 1.1 Gy in both HDR and LDR.

In this analysis, we compared urine from mice exposed to HDR 4.45 Gy irradiation to urine from respective controls at 2 days post-exposure. Using Welch's *t* test at *p* value of <0.05, we found more than 150 ions (ESI⁺ and ESI⁻ combined) whose urinary abundances change significantly post-irradiation. Same comparative analysis was carried out for urine collected from mice exposed to LDR 4.45 Gy. The results of this analysis yielded 90 significant

metabolites (Welch's *t* test, *p* value <0.05). It is important to note that both HDR and LDR exposures caused significant changes in the urinary metabolomic signature in mice. This is evident in Fig. 1a, c heatmaps that show clear separation of IR exposure metabolomic signature from that of controls for HDR and LDR cases, respectively. Furthermore, the volcano plots (Fig. 1b, d) show in red the individual metabolites that are affected significantly post-irradiation. As mentioned above and evident from the volcano plots, 4.45 Gy HDR irradiation resulted in higher number of significant metabolites than did 4.45 Gy LDR. In a separate statistical analysis, the urinary metabolomic signatures of 1.1 Gy HDR and LDR were studied and compared to that of the controls. Although the number of statistically significant metabolites was lower when compared to 4.45 Gy exposure, the overall metabolomic signature of the control mice stood visibly separate from those of 1.1 Gy HDR and 1.1 Gy LDR as shown in Fig. 2a PCA. The separation is also evident between 1.1 Gy HDR and 1.1 Gy LDR. This PCA shows that the metabolomic profiles of HDR and LDR samples are easily distinguishable even at the low dose of 1.1 Gy. This separation for the selected metabolites is further shown in the heatmap in Fig. 2b. Four distinct separations are seen in this heatmap. Box 1 highlights the metabolites that contribute the most to the separation of metabolomic profile of LDR samples from those of HDR and the controls. Box 2 shows that there are ions that show similar urinary excretion patterns between HDR and LDR groups but different from the controls. Box 3 shows examples of ions whose post-irradiation expression is unique to the HDR group, while box 4 shows ions with unique post-IR expression in LDR group. Although HDR and LDR groups share many ions that show similar patterns post-irradiation when compared to the controls (Table 1), there are ions whose urinary excretion is dose rate dependent (Table 2) and are unique to the HDR group or the LDR group. These ions show robust IR responses at 4.45 Gy as well as the lower dose of 1.1 Gy.

After establishing a general metabolomic profile for the different groups in the study, we narrowed our focus to identifying the metabolites that contributed the most to establishing the metabolomic profiles of LDR and HDR by calculating *p* values in a series of binary comparisons using the Welch's test. Those metabolites that fell below our predefined statistical significance threshold (*p* value <0.05) at both doses of 4.45 and 1.1 Gy were putatively identified and mapped out to various KEGG pathways. Several examples of urinary metabolites that display similar (top 3 bar graphs) and opposite (bottom 5 bar graphs) responses to dose rate are shown in Fig. 3 for both 4.45 and 1.1 Gy exposures. The y-axis in Fig. 3 represents the change in the relative urinary excretion of a metabolite post-irradiation with respect to its urinary excretion in control mice. The

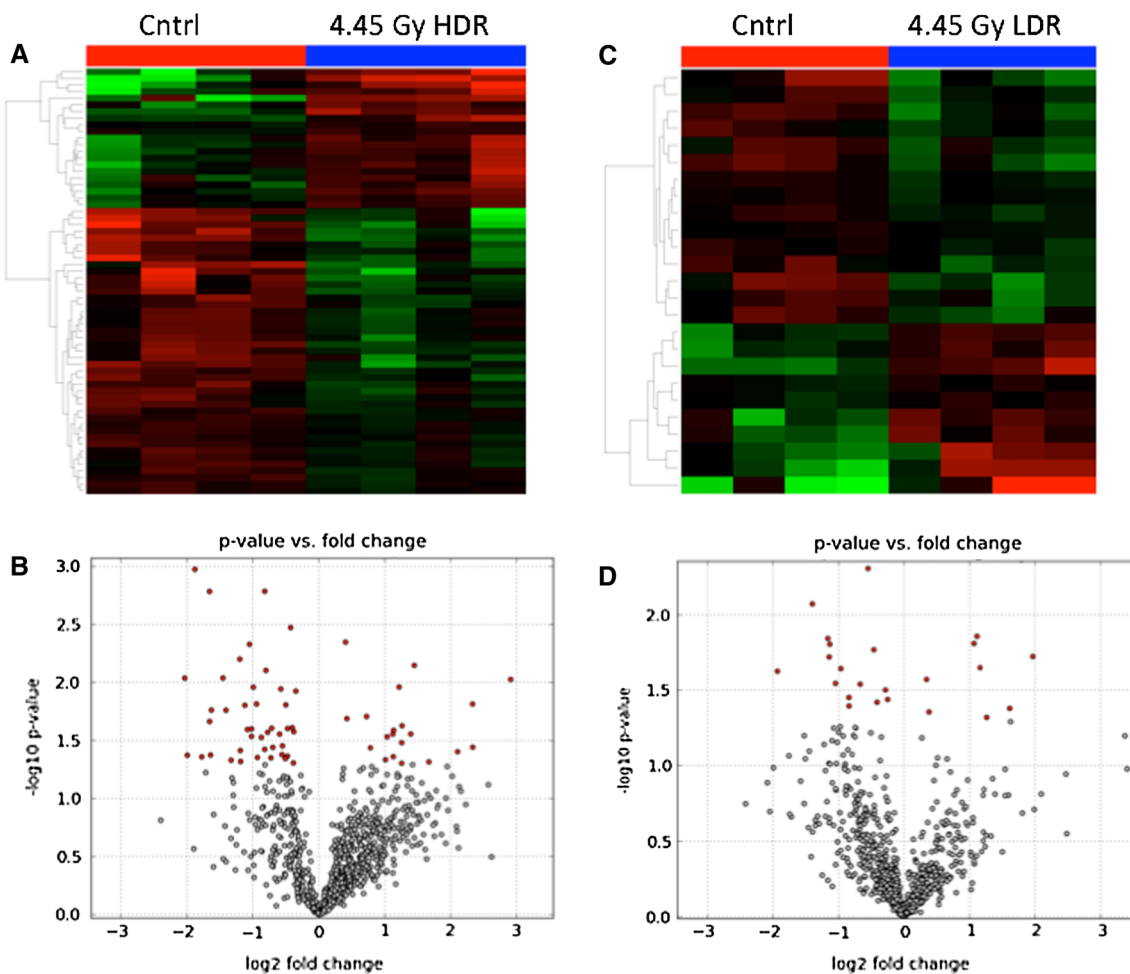


Fig. 1 The urinary metabolomic profile of urine after 4.45 Gy irradiation shows a distinct separation from that of urine from control mice at both dose rates ($n = 4$ per study group). **a** Heatmap generated in Metabolyzer shows a clear separation between the overall metabolomic signature of urine from mice exposed to 4.45 Gy HDR irradiation compared to urine from control mice. **b** Volcano plot created in Metabolyzer highlights in red the urinary metabolites that show statistically significant changes in their concentrations after

4.45 Gy HDR irradiation. **c** Heatmap created in Metabolyzer shows clear separation of urinary metabolomic profile of mice exposed to 4.45 Gy LDR irradiation compared to control mice. **d** Volcano plot depicts metabolites whose concentrations were determined to change statistically significantly (p value < 0.05) post-4.45 Gy LDR irradiation. Note that 4.45 Gy LDR irradiation shows in panels **c** and **d** fewer metabolites whose urinary abundances changed significantly post-irradiation than does 4.45 Gy HDR irradiation in panels **A** and **B**

putative identity of each metabolite was then validated by comparing its MS/MS fragmentation pattern to that of a pure chemical. The confirmed identities were then used to map out the metabolites to various metabolic pathways. For example, the ion with m/z value of 220.1175 ($[M + H]^+$) and retention time of 0.9807 was identified as pantothenic acid (PA). PA shows an increase in mice exposed to HDR and LDR irradiation when compared to respective controls. Similarly, the ion at m/z of 196.0963 ($[M + H]^+$) was identified as hexanoylglycine whose level increases post-irradiation in urine from both HDR and LDR mice. The ion at m/z of 191.0201 ($[M - H]^-$) was identified as citrate whose urinary excretion dropped in both HDR- and LDR-exposed mice post-irradiation. This is in accordance with our previous external γ -irradiation study and an internal

emitter exposure study where mice were injected with $^{137}\text{CsCl}$ (Goudarzi et al. 2013). Figure 3 also displays ions with varying behavior between HDR and LDR and their levels indicate a dose rate response. For instance, phenylacetylglutamine (m/z 194.0814) shows an increase in its urinary excretion after HDR exposure, while it shows a decrease after LDR exposure. The same is true for two carnitine species, tiglylcarnitine and hexanoylcarnitine. Hexanoylcarnitine was determined to show a similar decreasing trend in another LDR study with ^{137}Cs exposure (Goudarzi et al. 2013). Table 5 compares the urinary excretion patterns of several metabolites from this study, which also have been mentioned in other IR studies. For instance, the urinary excretion levels of citrate, hippuric acid, and uric acid in this study change in a similar fashion

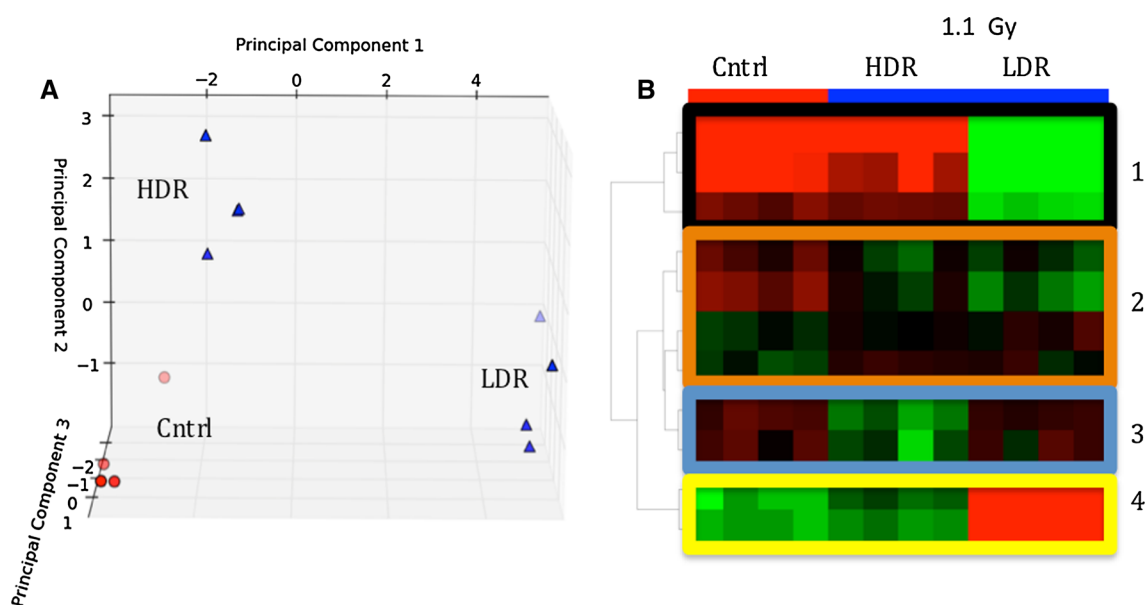


Fig. 2 **a** Principle component analysis (PCA) and **b** heatmap generated in Metabolyzer showing separation between controls (*red circles*) and 1.1 Gy irradiated samples (*blue triangles*). The heatmap highlights variations in urinary excretion levels of selected metabolites with respect to dose rate. *Box 1* shows the levels for metabolites that contributed the most to the separation of metabolomic profile of

LDR samples from those of HDR and the controls. *Box 2* shows that there are ions that show similar urinary excretion patterns between HDR and LDR groups but different from the controls. *Box 3* shows examples of ions whose post-irradiation expression is unique to the HDR group, while *box 4* shows ions with unique expression in LDR group

Table 1 Urinary dose-rate-independent metabolites 2 days post-4.45 Gy and 1.1 Gy irradiation

	<i>m/z</i> _RT	ID	Fold change HDR	Fold change LDR
1	153.0651_0.3355	N1-methyl-2-pyridone-5-carboxamide**	1.212	1.141
2	174.0553_2.6009	Quinaldic acid	1.350	1.370
3	220.1175_0.9027	Pantothenic acid**	1.890	1.710
4	178.0517_1.9308	Hippuric Acid**	1.085	1.028
5	136.0407_0.4442	Homocysteine	0.743	0.595
6	118.0860_0.3189	Valine**	1.034	1.163
7	191.0201_0.3574	Citrate**	0.697	0.765
8	188.0677_1.5133	NA	1.075	1.051
9	208.0610_1.9685	4-(2-Aminophenyl)-2,4-dioxobutanoic acid	1.120	1.139
10	196.0953_2.7491	Hexanoylglycine**	1.139	1.242
11	180.0659_1.9660	Tiglylglycine	1.554	1.289
12	190.0501_1.8074	Kynurenic acid**	0.895	0.655

The identities of metabolites designated with (**) were validated via MS/MS

as in other IR studies. Our data show perturbations in the levels of metabolites associated with energy metabolism such as citrate and α -ketoglutarate, tryptophan metabolism

Table 2 Urinary dose-rate-dependent metabolites 2 days post-4.45 Gy and 1.1 Gy irradiation

	<i>m/z</i> _RT	Putative ID	Fold change LDR	Fold change HDR
1	311.1234_2.4046	Gamma-glutamyltyrosine	0.915	2.581
2	244.1547_2.0563	Tiglylcarnitine**	0.473	2.440
3	194.0814_2.3822	Phenylacetylglycine**	0.882	1.488
4	260.1864_3.3971	Hexanoylcarnitine**	0.483	1.869
5	162.0550_2.2356	Indole-3-carboxylic acid**	0.622	0.948
6	216.1229_2.8090	Propenoylcarnitine**	0.620	1.288
7	221.0924_2.3216	5-Hydroxy-L-tryptophan**	0.810	3.730
8	162.0550_2.5029	Indole-3-carboxylic acid**	0.374	0.512

The identities of metabolites designated with (**) were validated via MS/MS

such as kynurenic acid and xanthurenic acid, and fatty acid β -oxidation such as acylcarnitines. In other words, both HDR and LDR exposures affect NAD⁺ degradation, coenzyme A synthesis, TCA cycle, and fatty acid metabolisms similarly. However, LDR and HDR have opposite effects on the urinary excretion levels of metabolites belonging to isoleucine catabolism, tryptophan metabolism,

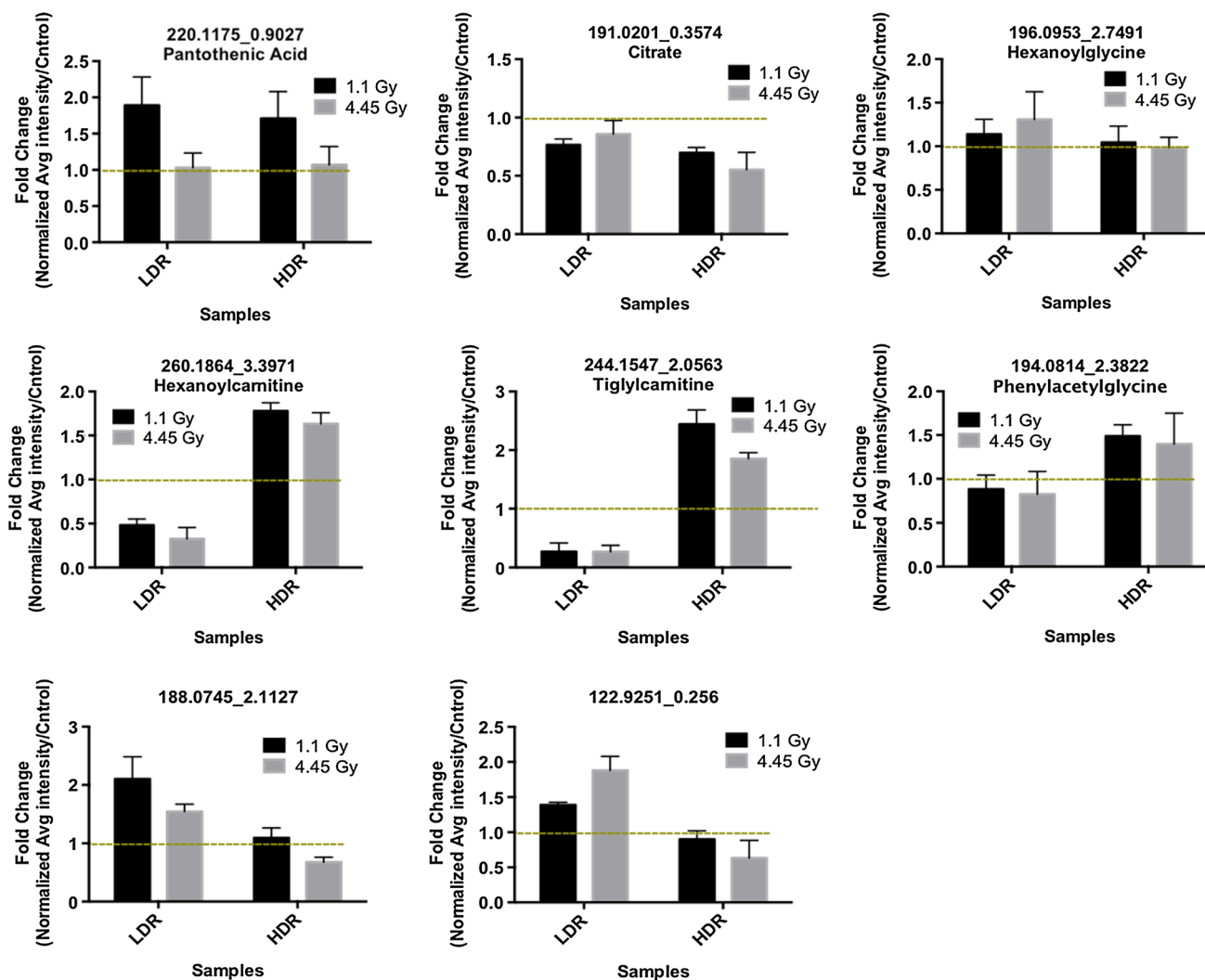


Fig. 3 Individual metabolite responses to dose rate. On top are three metabolites that do not show significant dose rate responses and at the bottom are those whose urinary excretion levels change with respect to dose rate 2 day post-irradiation. The dotted line marks fold change of 1, which in each graph represents no change in the abundance of

the metabolite pre- and post-irradiation. The identity of pantothenic acid, citrate, hexanoyleglycine, hexanoylecarnitine, tiglylcarnitine, phenylacetylglycine were validated via MS/MS fragmentation. No names could be assigned to metabolites at m/z of 188.0745 and 122.9251

and mitochondrial function. The last two metabolites in Fig. 3 could not be identified and validated via MS/MS; however, the change in their urinary abundances is statistically significant. The ion noted with m/z of 188.0745 and retention time of 2.1127 min is interesting because at 1.1 Gy, its levels increase after exposure in both HDR and LDR cases. However, at 4.45 Gy, its levels increase post-exposure only in the case of LDR, but decrease in HDR. This suggests that dose rate effects on its urinary excretion levels are secondary to dose effects. These results and the effects of dose rate on the urinary excretion of metabolites in Tables 1 and 2 were further confirmed in a separate experiment with four mice per study group. It is notable that fewer metabolites were found to be perturbed significantly in the urine of LDR

mice than in that of HDR mice. This is in accordance with the understanding that LDR exposure is less toxic than HDR exposure.

Time dependence

After establishing the effects of dose rate on the urinary excretion of several metabolites, we set out to determine how time could affect the urinary signatures of HDR and LDR. For this analysis, both our Metabolizer and RF were employed to determine whether the urinary metabolomic profile of urine from mice exposed to 4.45 Gy HDR radiation at 2 days post-exposure can be separated from that at 5 days post-irradiation. Similar analysis was performed for mice exposed to LDR irradiation. The graphical results of

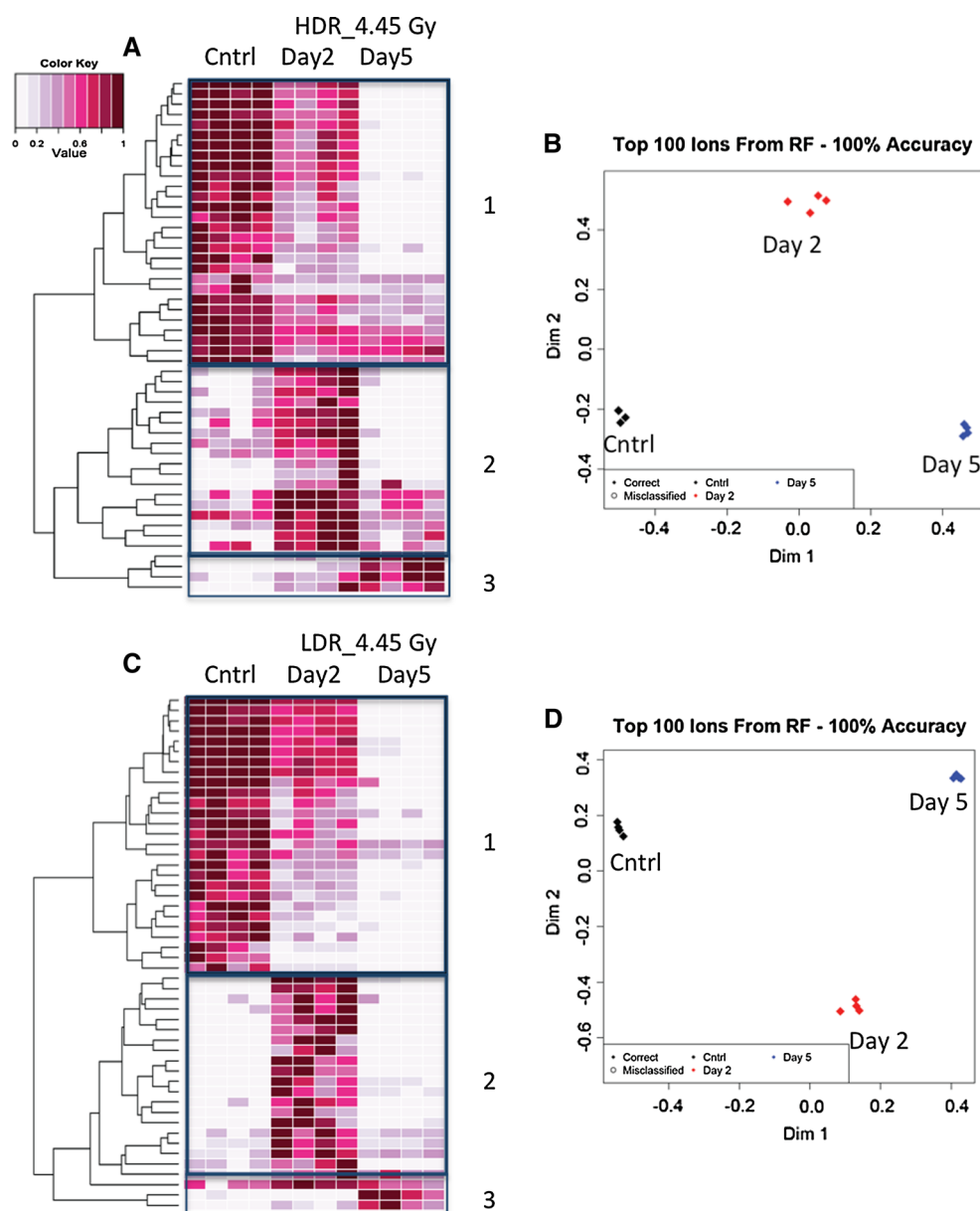


Fig. 4 Random Forests generated heatmaps (**a**, **c**) and MDS plots (**b**, **d**) show 50 metabolites, which contributed most significantly to establishing urinary metabolomic signatures for 4.45 Gy LDR and 4.45 Gy HDR exposures based on time passed after the initial exposure. Panel **a** heatmap shows a progressive decrease in the urinary levels of more than half of the selected 50 metabolites with respect to time post-4.45 Gy HDR exposure (*box 1*). *Box 2* in panel **a** shows several metabolites whose levels spiked at day 2 but dropped back to the levels seen in control mice at day 5 post-4.45 Gy HDR irradiation. *Box 3* shows a few metabolites whose levels do not show

any significant changes until 5 days post-exposure. These changes lead to distinct urinary metabolomic profiles for day 2 and day 5 post-irradiation as depicted in panel (**b**). Same analysis was carried out for 4.45 Gy LDR exposure. Panel **c** shows a progressive decrease in IR response for several metabolites in *box 1* as seen in panel A. *Box 2* shows an increase in the levels of metabolites at day 2, but these levels drop to their respective control levels by day 5. *Box 3* shows a few metabolites whose levels do not change until day 5. Panel **d** shows that these changes contribute to the differences in the overall metabolomic signature of day 2 and day 5

the analysis in RF are presented in Fig. 4 for 4.45 Gy and in Supplemental Figure 1 for 1.1 Gy as described below. Both HDR and LDR external γ exposures as expected created a time-dependence response in the urinary signature of exposed mice compared to that of sham-irradiated mice. Exposure to 4.45 Gy HDR irradiation clearly shows

a progressive decrease in the levels of many metabolites at 2 and 5 days post-exposure. This time-dependent decrease is readily evident in box 1 of Fig. 4a heatmap. Box 2 in the same figure shows several metabolites that show an increase in their urinary excretion levels at day 2, but these levels fall back to the control levels by day 5. Box 3 in

Table 3 HDR-specific metabolites showing persistent and/or progressive IR exposure responses

	<i>m/z</i> _RT	Putative ID	Day 2 fold change	Day 5 fold change
1	146.0826_2.9879	Isobutyrylglycine	0.745	0.271
2	194.0814_2.3822	Phenylacetylglycine**	1.488	1.664
3	297.1458_1.2573	NA	0.889	0.727
4	136.0621_1.6508	Adenine	0.367	0.029

The identity of metabolites designated with (**) was validated via MS/MS

Fold change at each time point was calculated by dividing the normalized relative urinary abundance of a metabolite at that time point post-exposure by that of its matched control

Fig. 4a shows a few metabolites that show late responses to IR at day 5. These changes in the metabolites' levels contribute to the separation of overall urinary profiles of day 2 and day 5 samples compared to controls in Fig. 4b. Similar patterns are seen with 4.45 Gy LDR exposure with the same distinct three groups shown in Fig. 4c heatmap and 4D MDS plot. Among the metabolites that show progressive decrease over time in their levels post-4.45 Gy irradiation are tryptophan pathway metabolites as well as a TCA cycle metabolite (Table 3). This is consistent with our previous observations with external beam γ exposure.

Although exposure to 1.1 Gy LDR irradiation has a more subtle effect on the urinary excretion profile of mice, there still are metabolites that showed distinct patterns with time as shown in supplemental Figure 1. Similar to Fig. 4, there are metabolites that show progressive decrease from day 2 to day 5 post-irradiation as well as metabolites that show IR responses at day 2 only or late responses at day 5. Box 3 in Supplemental Figure 1A and 1C shows metabolites whose urinary excretion levels persistently increase post-irradiation at day 2 and remain high by day 5. These changes in metabolite levels amount to separation of overall metabolomic profiles of urine from control and irradiated mice in Supplemental Figure 1B and 1D.

As the case with both 4.45 and 1.1 Gy doses, many of the metabolites show progressive time-dependent diminishing trends post-irradiation as highlighted in Supplemental Figure 1A and 1C as well as in Table 4. Riboflavin metabolism and coenzyme A metabolism in particular show significant drops in their urinary excretion levels of their intermediates. This observed time-dependence is in agreement with another IR study (Johnson et al. 2011) where urine was collected from 3 Gy γ -irradiated mice 1–3 days post-IR. In particular, urinary excretion of hexanoylglycine, alanine, and isovalerylglycine at days 2 and 3 was similar to what we observed in mice exposed to HDR radiation.

Table 4 LDR-specific metabolites displaying progressive decrease in their IR exposure responses

	<i>m/z</i> _RT	Putative ID	Day 2 fold change	Day 5 fold change
1	338.0878_2.2307	2,8-Dihydroxyquinoline-beta-D-glucuronide	0.621	0.549
2	659.2934_7.9268	NA	0.320	0.151
3	226.1442_3.0568	NA	0.593	0.450
4	206.045_1.5374	Xanthurenic acid**	0.881	0.658
5	377.1474_2.6141	Riboflavin**	0.691	0.410

The identity of metabolites designated with (**) was validated via MS/MS

Fold change at each time point was calculated by dividing the normalized relative urinary abundance of a metabolite at that time point post-exposure by that of its matched control

Discussion

Mass spectrometry-based metabolomics was used to study the often subtle yet unique changes in the urinary excretion profile of mice exposed to HDR and LDR radiation. As with our previous IR studies, there were no statistically significant changes in the excretion level of creatinine in control and irradiated mice, proof that kidney filtration was not affected by IR at these doses. The changes in mice body weight were comparable between the control and the irradiated groups. Thus, any change in energy metabolism is attributed to the systemic effects of IR.

As expected, exposure to 4.45 and 1.1 Gy irradiation resulted in changes in the urinary excretion of many metabolites at 2 days post-irradiation independent of dose rate. A total of 200 urinary ions (ESI⁺ and ESI⁻ modes combined) were found to be statistically significant in mice post-HDR exposure (both 1.1 and 4.45 Gy doses combined) and 107 ions post-LDR exposure when compared to respective control mice. The excretion levels of many of these metabolites were found to be similar between the HDR and LDR groups (Table 1; Figs. 3, 5). For instance, PA's urinary excretion level displayed a dose-rate-independent increase post-irradiation. PA has been associated with fatty acid β -oxidation and has been used as an oxidative stress marker. In addition, the TCA cycle metabolite, citrate, showed a consistent decrease in both HDR and LDR exposures as also noted in previous IR studies (Lanz et al. 2009; Tyburski et al. 2008). The urinary excretion of intermediates from valine and fatty acid metabolic pathways also showed a slight increase post-radiation in both HDR- and LDR-exposed mice. This indicates that the energy metabolism and fatty acid metabolism are general targets of IR exposure independent of dose rate. The fact

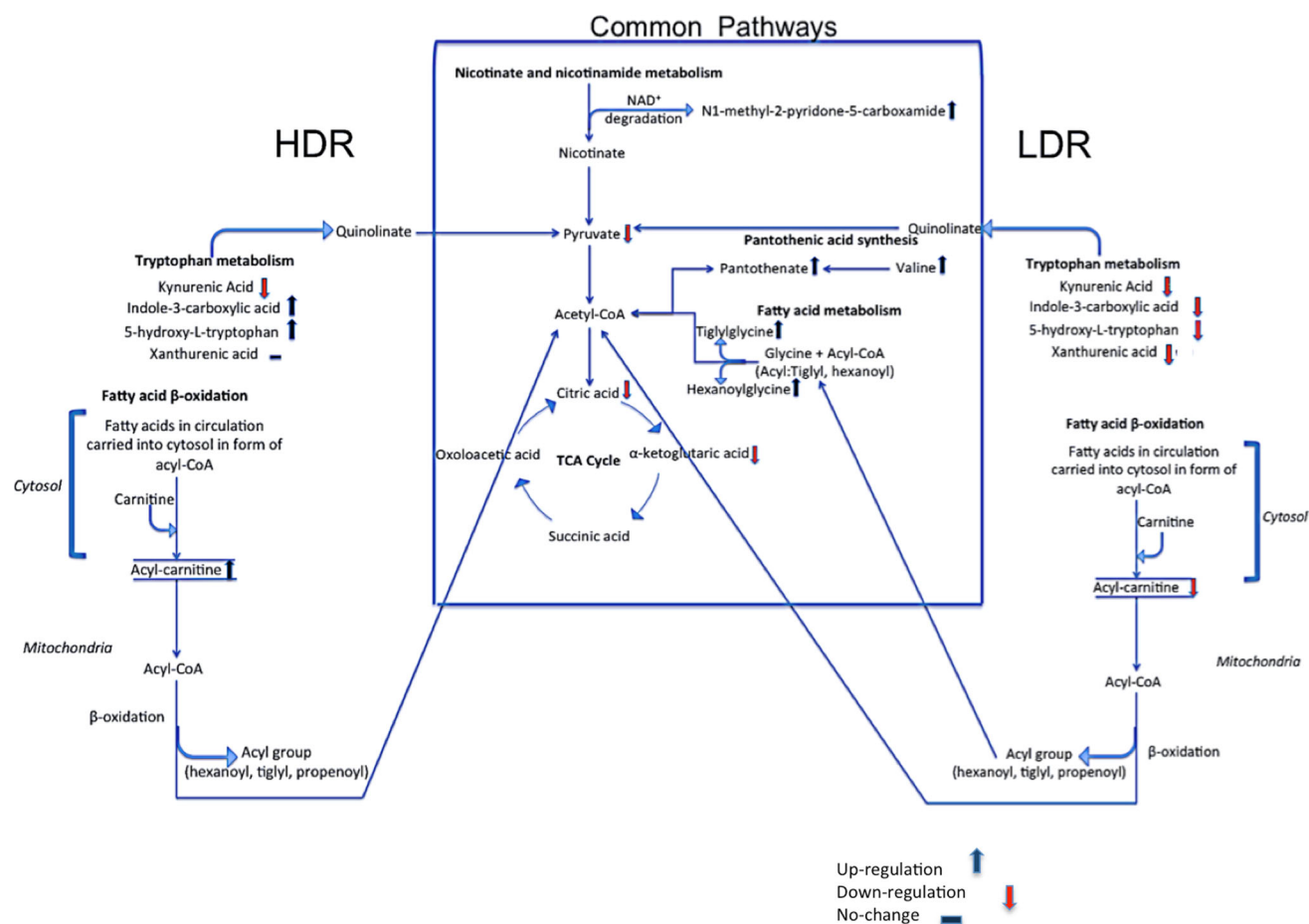


Fig. 5 Schematic of pathways that were determined to be affected significantly as a result of irradiation. The pathways within the box represent those that show similar perturbations with LDR and HDR independent of dose rate. Pathways to the left (HDR) and right (LDR) of the box are those whose metabolites show dose rate responses post-

irradiation. Notice that tryptophan and fatty β -oxidation pathways are both affected; however, the levels of their indicated metabolites changed in opposite direction post-irradiation with respect to dose rate

that many metabolites display a dose-rate-independent behavior follows the findings in an earlier transcriptomic analysis where a human myeloid cell line (ML-1) showed dose-rate-independent induction of several genes as early as 2 h post-irradiation (Amundson et al. 2003). These dose-rate-independent p53-regulated genes were determined to have roles in cell cycle progression. Although no direct comparisons can be drawn between this study and the study mentioned above, it is important to note that p53 and its effector genes are known to affect carbohydrate and fatty acid metabolism, mitochondrial function, and NAD biosynthesis (Berkers et al. 2013; Contractor and Harris 2012; Hallenborg et al. 2009). These pathways do appear as uniformly perturbed in HDR and LDR IR exposures in our study. They point to energy metabolism as the central network affected by IR exposure regardless of dose rate. However, both this study and that noted above revealed a highly complex network of gene and metabolic signaling with many dose-rate-dependent nodules. A closer look at

the urinary metabolomic signature of mice exposed to 4.45 Gy over 24 h and 1.1 Gy over 6 h revealed that the urinary levels of many metabolites from LDR-irradiated mice remained unchanged or slightly modulated compared to the urinary excretion levels of the same metabolites in HDR-irradiated mice. For instance, among 709 metabolites detected in the urine of 4.45 Gy exposed mice, only 90 were determined to change significantly (Welch's t test $p < 0.05$) in LDR, while this number was 170 in the urine from HDR-exposed mice in ESI⁺ mode. These numbers were substantially lower for the lower dose of 1.1 Gy: 45 for LDR and 70 for HDR. This indicates that the effects of LDR on the overall urinary metabolomic profile of mice were less pronounced than the effects of HDR irradiation. This is in accordance with long-established observations that LDR exposure is typically less toxic than an equivalent dose delivered in HDR manner (Hall and Giaccia 2006). A more in-depth look at the metabolites that contributed the most to the unique metabolomic profile of LDR exposure

as depicted in Figs. 1, 2 revealed subtle difference with HDR's metabolomic signature.

Thus, we further focused on metabolites that displayed a dose rate response at both 4.45 and 1.1 Gy doses and contributed the most to the separation of HDR and LDR metabolomic signatures at these two doses. This was made possible by utilizing our in-house program, Metabolyzer, where the irradiated mice (HDR and LDR) were grouped in a blinded sample set and compared against appropriate sham-irradiated mice. Those metabolites that fell within our predefined p value (<0.05) were chosen for further investigation and confirmation through a separate HDR/LDR exposure experiment. Table 2 shows examples of ions that showed unique dose rate responses. Among these ions are those belonging to tryptophan and carnitine metabolism. For instance, the urinary excretion of intermediates in the tryptophan metabolism and isoleucine catabolism was shown to markedly decrease in LDR-exposed mice and increase in HDR-exposed mice. Several carnitine species were found to be up-regulated 2 days post-HDR irradiation but decreased after LDR irradiation. This is in accordance with a recent study on mice exposed to $^{137}\text{CsCl}$ which mimics LDR conditions (1.95 Gy cumulative dose 2 days post-exposure) as shown in Table 5. It is important to note that the urinary signatures presented in this study are from mice that were exposed to irradiation 48 h prior to urine collection, while most urinary IR studies in the literature pertain to those where urine was typically collected just 24 h post-irradiation. This is an interesting observation that the urinary excretion levels of metabolites listed in Table 5 persist and remain steady during the first 48 h of exposure. Therefore, regardless of form of exposure and dose rate, the IR responses from these metabolites are persistently detectable. For example, the urinary abundance of hippuric acid and uric acid has been detected and determined to increase post-IR exposure in the three noted separate experiments in Table 5. The decreasing urinary levels of isovalerylglycine and citrate are also documented in the three cited studies. This shows that LDR exposure to a radionuclide causes the same perturbation in these metabolites as does exposure to external beam either at LDR or at HDR. It is important to note that the levels of these metabolites were confirmed in two different species (rats and mice), which is further proof to their persistence in IR responses (Johnson et al. 2011; Lanz et al. 2009). As more metabolites are studied and validated as IR exposure markers, a concrete and universal metabolomic signature will become available to the first responders of radiologic and nuclear events. This persistent urinary IR signature may have utility in triaging potentially exposed populations since access to screening may not be immediate.

We further investigated the persistency of metabolic signal in the urine of mice in this study by examining the excretion of selected metabolites 5 days post-exposure in LDR and HDR groups compared to that of metabolites 2 days post-exposure. It has been shown in previous studies that urinary excretion of hexanoylglycine and isovalerylglycine 1–3 days post-3 Gy irradiation (HDR) is time dependent where that of isovalerylglycine decreased and that of hexanoylglycine increased (Johnson et al. 2011). Statistical analysis of our data revealed a similar pattern in these ions. We also found an intermediate involved in energy metabolism, kynurenic acid, showing diminishing levels with time after 1 Gy HDR irradiation as well as indole-3-carboxylic acid, which is an important player in tryptophan metabolism. An ion at m/z of 377.1474 confirmed as riboflavin via MS/MS fragmentation was found in decreasing levels in the urine of mice exposed to LDR irradiation. The urinary level of a putatively identified glucuronide species was also observed to grossly decrease by time post-LDR exposure. Figure 4 shows how urine collected 2 days post-irradiation can be distinguished from urine collected 5 days post-exposure. In addition, Tables 3 and 4 show a few ions whose urinary excretion levels change with time post-HDR and post-LDR irradiation, respectively.

Collectively, the data gathered in this study suggest that LDR and HDR external beam irradiation has common metabolic targets in mice. In particular, energy metabolism and fatty acid metabolism are affected in both cases as also shown in previous studies (Johnson et al. 2011; Laiakis et al. 2012; Tyburski et al. 2008) and further impacted by dose rate and time lapsed between first IR exposure and biofluid collection. Figure 5 shows several pathways whose one or more metabolites have been determined in this study to be statistically significantly perturbed in the urine of mice exposed to IR at HDR and LDR. The box in the middle of this figure displays the pathways whose metabolites change similarly in the case of HDR and LDR exposure. Several of the metabolites in this box have also been mentioned in other IR studies with external beam and radionuclides. Hence, the metabolites specified in this box may be persistent IR markers that can be used for determining a solid metabolomic signature for IR exposure regardless of type of exposure or dose rate. To either side of this center box are metabolites that showed different urinary abundances based on dose rate. For instance, the urinary signal from xanthurenic acid, a tryptophan pathway metabolite, was determined to be significantly depleted after LDR exposure as also mentioned in our previous ^{137}Cs exposure study, while its levels remain unchanged post-HDR exposure. The urinary excretion levels of two other tryptophan pathway metabolites, indole-3-carboxylic

Table 5 Comparison of changes in urinary excretion of several IR metabolite markers in various HDR and LDR experiments

<i>m/z</i> _RT	Exposure	Change in Urinary Excretion			
		LDR 1.1 Gy (3.09 mGy/ min) 48 h post-exposure	HDR 1.1 Gy 48 h post- exposure	¹³⁷ Cs Exposure 1.95 Gy (cumulative) 48 h post-exposure	γ Exposure 1 Gy 24 h post- exposure
1 206.045_1.5374	Xanthurenic acid	↓	No change	↓	–
2 244.1547_2.0563	Tiglylcarnitine	↓	↑	↓	–
3 260.1864_3.3971	Hexanoylcarnitine	↓	↑	↓	–
4 180.0659_1.966	Tiglylglycine	↑	↑	↑	–
5 178.0517_1.9308	Hippuric acid	↑	↑	↑	↑ ¹
6 158.0831_1.5708	Isovalerylglycine	↓	↓	↓	↓ ¹
7 191.0201_0.3574	Citrate	↓	↓	↓	↓ ^{2,3}
8 167.0215_0.326	Uric acid	↑	↑	↑	↑ ^{2,4}
9 145.0153_0.3143	α-ketoglutaric acid	↓	↓	↓	↓ ²

¹³⁷ Cs exposure refers to a study where mice were injected intraperitoneally with ¹³⁷CsCl. Urine was collected 2 days post-injection and the body cumulative dose was counted to be at 1.95 Gy

¹ Johnson et al. (2011)

² Lanz et al. (2009)

³ Tyburski et al. (2008)

⁴ Laiakis et al. (2012)

acid and 5-hydroxy-L-tryptophan, have been shown to decrease in this study post-1.1 Gy LDR irradiation. This is different from what we observed with HDR 1.1 Gy irradiation and what has been reported in literature as shown in Table 4. The data also indicate that the changes in the levels of urinary metabolites are less pronounced with LDR irradiation than with HDR. This finding is intriguing because tryptophan metabolism is linked to the central energy metabolic pathways and the TCA cycle through pyruvate and is important in energy metabolism. Figure 5 also shows three acylcarnitines to be down-regulated post-LDR exposure, while the same metabolites were found to be at higher abundances in the urine of mice post-HDR exposure. This result was compared to a recent human total body irradiation study (Laiakis et al. 2014), where the authors observed a decrease in the urinary excretion levels of several acylcarnitines, octanoylcarnitine, acetylcarnitine, and decanoylcarnitine, 6 h after 1.25 Gy total body irradiation. This decrease is consistent with what we observed with LDR irradiation in this study. Acylcarnitines play a crucial role in fatty acid β-oxidation. Therefore, the result may indicate that fatty acid β-oxidation is a general target of external beam irradiation in both mice and humans and is further impacted by dose rate in mice. The Laiakis et al. report also highlighted the increase in uric acid post-irradiation, which agrees with what we observed in mice in this study. Uric acid is the end product of purine metabolism and is found at elevated levels under increased oxidative stress. The results of these two studies showed that

irradiation affected the urinary excretion of these metabolites in both species similarly and independent of dose rate in mice. Together, these results suggest that although there exist some differences in the urinary metabolomic profiles of LDR and HDR exposure, there are similarities across species in terms of robust and persistent radiation-induced metabolic responses.

Conclusion

The results of this study provide new insight into the effects of dose rate on metabolism and its manifestation in urinary output of C57BL/6 mice. As expected, exposure to external beam γ-irradiation regardless of dose rate perturbed energy metabolism, fatty acid oxidation, and amino acid metabolism. This is in accordance with previous gene expression and transcriptomics analysis (Amundson et al. 2003). Dose rate is speculated to modulate the magnitude of metabolic perturbations and the targets within metabolic pathways. It is important to note that at low doses such as 1 Gy, the differences between the urinary metabolomic profiles of LDR- and HDR-exposed mice are subtle. However, today's mass spectrometers have the sensitivity and accuracy to measure even subtle changes in the abundance of a metabolite. This makes mass spectrometry the platform of choice for detecting changes in urinary excretion of metabolites even at non-lethal doses.

Acknowledgments This study was supported by the National Institute of Health (National Institute of Allergy and Infectious Diseases) grant U19 A1067773. The authors would like to thank Georgetown University's Proteomic and Metabolomics Shared Resources, NIH P30 CA51008, for providing access to mass spectrometry and related resources. We would also like to acknowledge the efforts of Steven Strawn in obtaining pure chemical standards and Yue Luo and Rajbir Sohi in mass spectrometry.

References

- Amundson SA, Lee AL, Koch-Paiz CA, Bittner ML, Meltzer P, Trent JM, Fornace AJ Jr (2003) Differential responses of stress genes to low dose-rate gamma-irradiation. *Mol Cancer Res* 1(445–52):445–452
- Berkers CR, Maddocks ODK, Cheung EC, Mor I, Vousden KH (2013) Metabolic regulation by p53 family members. *Cell Metab* 18(5):617–633
- Contractor T, Harris CR (2012) p53 negatively regulates transcription of the pyruvate dehydrogenase kinase Pdk2. *Cancer Res* 72:560–567
- Elkind MM, Sutton H (1959) X-ray damage and recovery in mammalian cells in culture. *Nature* 184:1293–1295
- Evans HH, Horng MF, Mencl J, Glazier KG, Beer JZ (1985) The influence of dose rate on the lethal and mutagenic effects of X-rays in proliferating L5178Y cells differing in radiation sensitivity. *Int J Radiat Biol Relat Stud Phys Chem Med* 47:553–562
- Goudarzi M, Weber W, Mak TD, Chung J, Doyle-Eisele M, Melo D, Brenner D, Guilmette R, Fornace AJ Jr (2013) Development of urinary biomarkers for internal exposure by cesium-137 using a metabolomics approach in mice. *Rad Res* 181:54–64
- Hall EJ, Giaccia AJ (2006) *Radiobiology for the radiologist*. Lippincott Williams & Wilkins, London
- Hallenborg P, Feddersen S, Madsen L, Kristiansen K (2009) The tumor suppressors pRB and p53 are regulators of adipocyte differentiation and function. *Expert Opin Ther Targets* 13:35–46
- Johnson CH, Patterson AD, Krausz KW, Lanz C, Kang DW, Luecke H, Gonzalez FJ, Idle JR (2011) Radiation metabolomics. 4. UPLC-ESI-QTOFMS-Based metabolomics for urinary biomarker discovery in gamma-irradiated rats. *Radiat Res* 175(4):473–484
- Kanehisa M, Goto S (2000) KEGG: kyoto encyclopedia of genes and genomes. *Nucleic Acids Res* 28:27–30
- Laiakis EC, Hyduke DR, Fornace AJ (2012) Comparison of mouse urinary metabolic profiles after exposure to the inflammatory stressors γ radiation and lipopolysaccharide. *Radiat Res* 177:187–199
- Laiakis EC, Mak TD, Anizan S, Amundson SA, Barker CA, Wolden SL, Brenner DJ, Fornace AJ (2014) Development of a metabolomic radiation signature in urine from patients undergoing total body irradiation. *Radiat Res* 181:350–361
- Lanz C, Patterson AD, Slavik J, Krausz KW, Ledermann M, Gonzalez FJ, Idle JR (2009) Radiation metabolomics. 3. Biomarker discovery in the urine of gamma-irradiated rats using a simplified metabolomics protocol of gas chromatography-mass spectrometry combined with random forests machine learning algorithm. *Radiat Res* 172(2):198–212
- Mak TD, Laiakis EC, Goudarzi M, Fornace AJ Jr (2014) Metabolyzer: a novel statistical workflow for analyzing postprocessed LC-MS metabolomics data. *Anal Chem* 86:506–513
- Nagasawa H, Chen DJ, Strniste GF (1992) Response of X-ray-sensitive CHO mutant cells to γ radiation. I. Effects of low dose rates and the process of repair of potentially lethal damage in GI phase. *Radiat Res* 118:559–567
- Oakberg EF, Clark E (1961) Effect of dose and dose rate on radiation damage to mouse spermatogonia and oocytes as measured by cell survival. *J Cell Comp Physiol* 58:173–182
- Tyburski JB, Patterson AD, Krausz KD, Slavik J, Fornace AJ Jr, Gonzalez FJ, Idle JR (2008) Radiation metabolomics. 1. Identification of minimally invasive urine biomarkers for gamma-radiation exposure in mice. *Radiat Res* 170(1):1–14